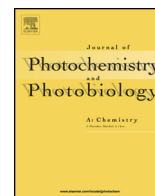




Contents lists available at ScienceDirect

Journal of Photochemistry and Photobiology A: Chemistry

journal homepage: www.elsevier.com/locate/jphotochem

A tetraphenylethylene-based “turn on” fluorescent sensor for the rapid detection of Ag⁺ ions with high selectivity



Yong Li, Huijuan Yu, Guang Shao*, Feng Gan*

School of Chemistry and Chemical Engineering, Sun Yat-Sen University, Guangzhou 510275, PR China

ARTICLE INFO

Article history:

Received 20 October 2014

Received in revised form 9 December 2014

Accepted 26 December 2014

Available online 30 December 2014

Keywords:

Ag⁺

Fluorescence

Sensor

Tetraphenylethylene

AIE

ABSTRACT

A new fast-responsive “turn on” fluorescent sensor for Ag⁺ was successfully developed by taking advantage of the aggregation-induced emission (AIE) property of tetraphenylethylene motif with a detection limit of 8.74×10^{-7} M. The sensor exhibits highly selective and sensitive recognition toward Ag⁺ ions over the other 12 metal ions due to the high electrophilic and thiophilic character of Ag⁺ ions. The ¹H NMR titration and dynamic light scattering (DLS) spectra conclude that the binding of the sensor with Ag⁺ ions forms fluorescent nanoaggregates in aqueous media due to its AIE enhancement. A stoichiometric ratio (1:2) of the sensor and Ag⁺ was determined by a Job's plot.

© 2015 Published by Elsevier B.V.

1. Introduction

Silver is widely used in many industrial fields such as chemistry, pharmacies, photography, and electrical industries [1,2], thus a large amount of silver is discharged into the environment annually from industrial wastes in a variety of chemical forms. As silver ions (Ag⁺) can bond with various metabolites such as amine, imidazole and carboxyl groups in enzymes/proteins, it will lead to enzymes/proteins inactivation and bio-accumulation [3,4]. Thus, it is an important research field to develop sensitive and selective methods for detecting and monitoring trace amounts of Ag⁺ in various media.

Some traditional methods such as ion-selective electrodes [5], inductively-coupled plasma emission mass spectrometry [6,7], atomic absorption spectrometry [8] and electrochemical method [9] have been employed to detect trace level of Ag⁺, but most of them are expensive and time-consuming. Recently, researchers are interested in developing fluorescence probes for Ag⁺, which only need simple instruments and are easy to operate. Unlike other transition metal ions such as Cu²⁺ [10] and Fe²⁺, Ag⁺ is spectroscopically and magnetically silent because of its [Kr] 4d¹⁰5s⁰ quenching electron configuration [11,12]. As a result, it is a challenge to design a fluorescence “turn on” sensor to discriminate Ag⁺ from other chemically similar ions [13].

In recent years, AIE materials have drawn considerable research attention because of their applications in various fields, such as organic light emitting devices and sensors [14–16]. The restricted intramolecular rotation (RIR) is the main mechanism for AIE effect [17]. These materials display excellent fluorescence stability and overcome the drawback of traditional organic dyes [18,19]. Although Liu et al. [20] reported sensors for Ag⁺ based on tetraphenylethylene, their applications are limited due to the quenching interference of Hg²⁺.

Herein, we developed a new fluorescence “turn on” sensor for the detection of Ag⁺. The sensor (TPE-4DDC) (Scheme 1) with AIE characteristics shows a strong anti-interference capacity for various metal ions. The selective dimethyldithiocarbamate (DDC) moiety can bind with Ag⁺ based on the electrophilic and thiophilic character of Ag⁺ [21,22]. As a result, the sensor is non-emissive in solution but becomes strongly emissive after addition of Ag⁺.

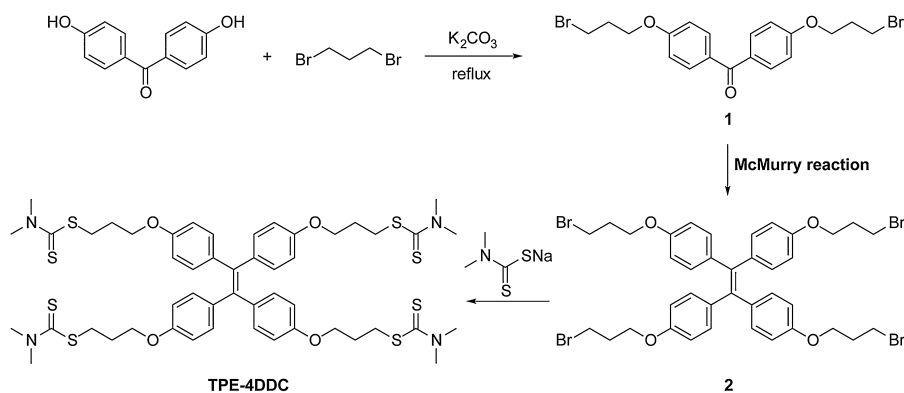
2. Experimental methods

2.1. Chemicals and instruments

Unless otherwise noted, reagents were purchased from commercial supplies and used without further purification. Solvents and twice-distilled water were purified by standard methods. All metal ions solutions were prepared from their nitrate salts (AgNO₃, Hg(NO₃)₂, Pb(NO₃)₂, Co(NO₃)₂, Cu(NO₃)₂, Zn(NO₃)₂, Mg(NO₃)₂, Ca(NO₃)₂, Cr(NO₃)₃, Al(NO₃)₃, Fe(NO₃)₃, Ba(NO₃)₂ and Ni(NO₃)₂) in distilled water with a concentration of

* Corresponding authors. Tel.: +86 20 84110918; fax: +86 20 84110918.

E-mail addresses: shaog@mail.sysu.edu.cn (G. Shao), cesgf@mail.sysu.edu.cn (F. Gan).



Scheme 1. Synthesis of TPE-4DDC.

10 mM, respectively. The different Ag^+ solutions were prepared from AgClO_4 , AgCF_3SO_3 , AgNO_3 , AgBF_4 and AgOAc in distilled water, with a concentration of 10 mM, respectively. All UV–vis absorption and fluorescence spectra were measured in 20 mM 4-(2-hydroxyethyl)-1-piperazineethanesulfonic acid (HEPES) buffer solution (pH=7.0) unless otherwise noted. TLC analyses were performed on silica gel plates and column chromatography was conducted over silica gel (200–300 mesh).

The melting points were measured on an YRT-3 (Tianjin Xintian Optical Analytical Instruments Co., Ltd.) melting point apparatus without calibration. ^1H and ^{13}C NMR spectra were recorded at 25 °C on a Bruker 300 MHz or 400 MHz nuclear magnetic resonance spectrometer. Chemical shifts were reported relative to Me_4Si for ^1H and ^{13}C NMR spectra. Mass spectra were obtained from DQ (Thermo) and LCMS-2010A (Shimadzu). High-resolution mass spectrometry (HRMS) was performed on MAT95XP (Thermo). FT-IR spectra were recorded as KBr pellets on an IR-Nicolet Avatrar 330 spectrometer at room temperature. UV–vis absorption spectra were characterized by a UV-3150 spectrophotometer (Shimadzu) at room temperature. Fluorescence emission spectra were investigated by a RF-5301 (Shimadzu) at room temperature. Quantum yields were measured by a photoluminescence spectrometer (FLS-980, Edinburgh Instruments Ltd) at room temperature.

2.2. Synthesis

2.2.1. Synthesis of compound 1

A mixture of 4,4'-dihydroxybenzophenone (5.00 g, 23.3 mmol), 1,3-dibromopropane (14.20 g, 70.0 mmol) and K_2CO_3 (9.50 g, 70.0 mmol) in dry DMF (50 mL) was stirred under Ar atmosphere at room temperature for 24 h. After reaction, the resulting mixture was extracted with ethyl acetate (3×20 mL). Then the organic phase was washed with saturated brine (20 mL) and dried over Na_2SO_4 . After removing solvent under reduced pressure, the crude product was purified by column chromatography on silica gel using petroleum ether (60–90 °C) and EtOAc (v/v, 10/1) as eluent. A white powder of compound 1 was obtained in a yield of 26.0% (2.36 g). mp = 62.4–63.7 °C; ^1H NMR (300 MHz, CDCl_3), δ : 7.76 (d, J = 8.7 Hz, 4H), 6.94 (d, J = 8.7 Hz, 4H), 4.18 (t, J = 5.8 Hz, 4H), 3.61 (t, J = 6.3 Hz, 4H), 2.39–2.31 (m, 4H). ^{13}C NMR (75 MHz, CDCl_3), δ : 194.74, 161.73, 132.06, 130.79, 113.87, 65.52, 32.23, 29.74. MS (ESI) m/z : $[\text{M} + \text{Na}]^+$ Calcd for $\text{C}_{19}\text{H}_{20}\text{Br}_2\text{O}_3\text{Na}$: 479.0; Found: 478.7.

2.2.2. Synthesis of compound 2

A suspension of TiCl_4 (0.78 mL, 7.0 mmol) and Zn powder (0.92 g, 14.0 mmol) in 35 mL of dry THF was refluxed under Ar atmosphere for 2 h. A solution of compound 1 (1.60 g, 3.50 mmol) in dry THF

(15 mL) was added to the suspension of the titanium reagent and the reaction was refluxed for 10 h at 80 °C. The reaction mixture was cooled to room temperature and a 10% aqueous K_2CO_3 solution (50 mL) was added. The dispersed insoluble material was removed by vacuum filtration using a celite pad after vigorous stirring for 5 min. The organic layer was separated and the aqueous layer was extracted with ethyl acetate (3×20 mL). Then the combined organic phase was dried over Na_2SO_4 and concentrated in vacuum. The crude product was purified by column chromatography on silica gel using petroleum ether (60–90 °C)/EtOAc/ CH_2Cl_2 (v/v/v, 10/1/1) as eluent. The product was obtained as white powder in a yield of 57.0% (0.88 g). mp = 118.2–120.1 °C. ^1H NMR (400 MHz, CDCl_3), δ : 6.91 (d, J = 8.8 Hz, 8H), 6.62 (d, J = 8.8 Hz, 8H), 4.01 (t, J = 5.8 Hz, 8H), 3.56 (t, J = 6.4 Hz, 8H), 2.29–2.23 (m, 8H). ^{13}C NMR (100 MHz, CDCl_3), δ : 156.84, 138.29, 136.98, 132.48, 113.57, 65.05, 32.40, 30.05. MS (EI) m/z : $[\text{M}]^+$ Calcd for $\text{C}_{38}\text{H}_{40}\text{Br}_4\text{O}_4$: 880; Found: 880. HRMS (EI) m/z : $[\text{M}]^+$ Calcd for $\text{C}_{38}\text{H}_{40}\text{Br}_4\text{O}_4$: 879.9614; Found: 879.9627.

2.2.3. Synthesis of TPE-4DDC

A mixture of compound 2 (0.41 g, 3.50 mmol), sodium dimethyldithiocarbamate (0.40 g, 14.00 mmol) and KI (0.14 g, 1.4 mmol) in acetone (15 mL) was refluxed for 20 h under Ar atmosphere. After the reaction mixture was cooled to room temperature, the solvent was evaporated under reduced pressure. The product was purified by column chromatography on silica gel using petroleum ether (60–90 °C)/EtOAc (v/v, 5/1) as eluent. A white powder of TPE-4DDC was obtained in a yield of 41% (0.18 g). mp = 134.4–136.4 °C. ^1H NMR (300 MHz, $\text{DMSO}-d_6$), δ : 6.82 (d, J = 8.1 Hz, 8H), 6.67 (d, J = 8.1 Hz, 8H), 3.96–3.92 (m, 8H), 3.44 (s, 12H), 3.33–3.28 (m, 20H), 2.05–2.01 (m, 8H). ^{13}C NMR (75 MHz, $\text{DMSO}-d_6$), δ : 194.80, 156.45, 137.82, 136.15, 131.81, 113.60, 65.94, 44.85, 41.24, 33.35, 28.13. IR (cm^{-1}): 3428.51, 2921.74, 1605.09, 1506.30, 1374.29, 1290.23, 1242.17, 1172.56, 1143.28, 1038.79, 983.32. MS (ESI) m/z : $[\text{M} + \text{H}]^+$ Calcd for $\text{C}_{50}\text{H}_{65}\text{N}_4\text{O}_4\text{S}_8$: 1041.2; Found: 1041.0. HRMS (ESI) m/z : $[\text{M} + \text{H}]^+$ Calcd for $\text{C}_{50}\text{H}_{65}\text{N}_4\text{O}_4\text{S}_8$: 1041.27660; Found: 1041.27691.

3. Results and discussion

3.1. AIE studies

The AIE properties of TPE-4DDC were examined by studying the fluorescence behavior of its diluted solution in H_2O /THF under different H_2O fractions (Fig. 1). TPE-4DDC has four phenyl rings with intramolecular rotations that quench its emission, however, when it turns into an aggregated form, the intramolecular coordinations occur. Accordingly, the intramolecular rotations are restricted and the non-radiative decay channels are hindered. As a result, TPE-4DDC

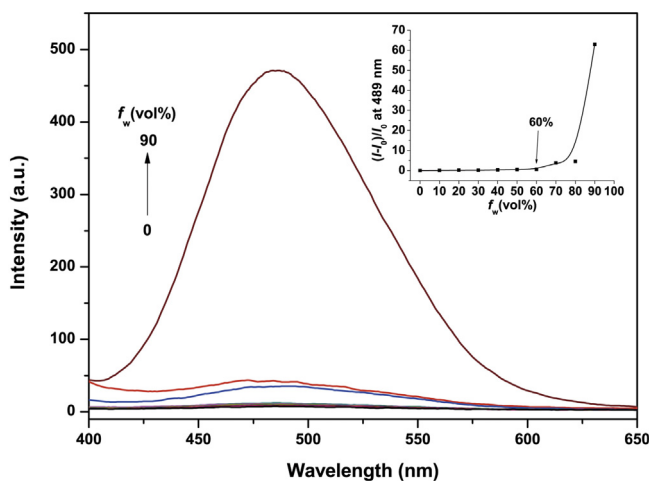


Fig. 1. Fluorescence spectra of TPE-4DDC (10.0 μM) in $\text{H}_2\text{O}/\text{THF}$ mixtures with different H_2O fractions (f_w) at 25 $^\circ\text{C}$. Inset: Plot of $(I - I_0)/I_0$ values versus f_w in $\text{H}_2\text{O}/\text{THF}$ mixtures ($\lambda_{\text{ex}} = 353 \text{ nm}$, $\lambda_{\text{em}} = 488 \text{ nm}$; slit: 3 nm, 5 nm).

becomes active for emission. Plot of fluorescence intensity versus wavelength shows the fluorescence behavior of TPE-4DDC while changing the H_2O portion of solution from 0% to 90%. TPE-4DDC is non-emissive when dissolved in a good solvent (THF) as isolated single molecules. However, once the H_2O (a poor solvent) fraction exceeds the limit of 60%, the fluorescence intensity starts to increase drastically. When the H_2O fraction was increased from 0% to 90%, the change ratio of fluorescent intensity $((I - I_0)/I_0)$, where I_0 is the initial fluorescence intensity, and I is the fluorescence intensity after addition of H_2O . (inset of Fig. 1) shows an approximate 63-fold enhancement. Owing to the condition of critical non-fluorescent emission, the solution with 60% H_2O fraction was chosen as the media to explore the next experiments of selective and sensitive monitoring.

3.2. Spectroscopic titrations of TPE-4DDC by Ag^+

As shown in Fig. 2, we investigated the fluorescence emission changes ($\lambda_{\text{ex}} = 353 \text{ nm}$) of TPE-4DDC (40.0 μM) in the presence of Ag^+ in $\text{H}_2\text{O}/\text{THF}$ (v/v, 6/4) at room temperature. With the addition of Ag^+ , the emission intensity of TPE-4DDC gradually increased at

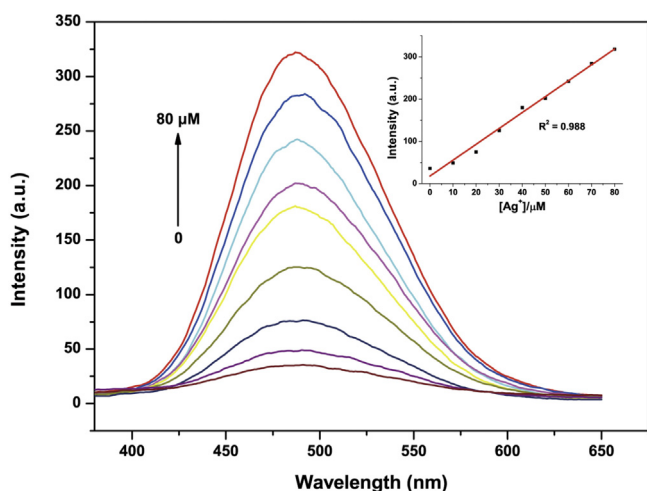


Fig. 2. Fluorescence emission changes of TPE-4DDC (40.0 μM) upon addition of Ag^+ (nitrate salt) in $\text{H}_2\text{O}/\text{THF}$ (v/v, 6/4) containing HEPES buffer (20 mM, pH = 7.0) at 25 $^\circ\text{C}$: $[\text{Ag}^+] = 0, 10.0, 20.0, 30.0, 40.0, 50.0, 60.0, 70.0,$ and $80.0 \mu\text{M}$ ($\lambda_{\text{ex}} = 353 \text{ nm}$, $\lambda_{\text{em}} = 488 \text{ nm}$; slit: 1.5 nm, 15 nm).

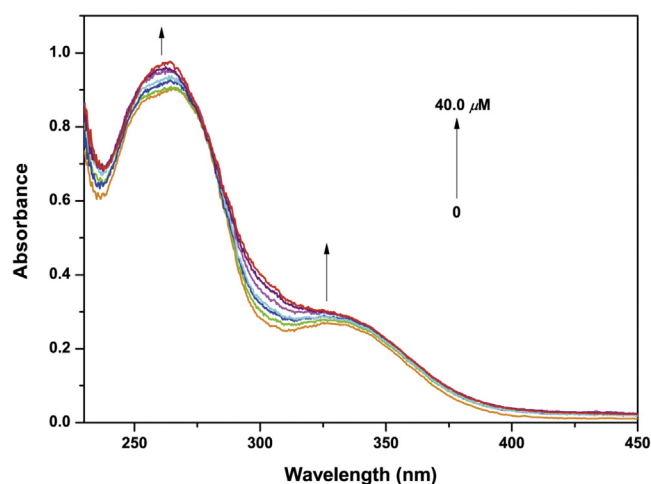


Fig. 3. UV-vis spectra of TPE-4DDC (10.0 μM) upon titration of Ag^+ (0–40.0 μM) in $\text{H}_2\text{O}/\text{THF}$ (v/v, 6/4) containing HEPES buffer (20 mM, pH = 7.0).

488 nm. Similarly, fluorescence quantum yields (Φ_F) of TPE-4DDC in $\text{H}_2\text{O}/\text{THF}$ (v/v, 6/4) increased, which were measured by an integrated sphere system. In the absence of Ag^+ , the Φ_F value of TPE-4DDC is merely 0.92%. Whereas in the presence of Ag^+ (2.0 eq), its Φ_F value rises to 7.38%.

The detection limit was calculated to be $8.74 \times 10^{-7} \text{ M}$ from the fluorescence intensity changes upon the addition of Ag^+ in the range of 0–16 μM (Fig. S1). The detection limit was calculated with the equation: detection limit = $3 \sigma_{\text{bi}}/m$, where σ_{bi} is the standard deviation of blank measurements and m is the slope of the intensity versus Ag^+ concentration [23]. The UV-vis absorption was also recorded upon the addition of Ag^+ (Fig. 3). The absorptions around 264 nm and 328 nm increased gradually with the increasing amounts of Ag^+ . Simultaneously, a long absorption tail above 400 nm was observed. The molar absorption coefficient values (ϵ_{max}) of TPE-4DDC (10.0 μM) in the absence and presence of Ag^+ (2.0 eq) in $\text{H}_2\text{O}/\text{THF}$ (v/v, 6/4) are $9.05 \times 10^4 \text{ L mol}^{-1} \text{ cm}^{-1}$ (265 nm) and $9.56 \times 10^4 \text{ L mol}^{-1} \text{ cm}^{-1}$ (263 nm), respectively, calculated at the respective λ_{max} value. The larger molar absorption coefficient indicates its strong ability to absorb light. These spectral changes are in agreement with the aggregation of TPE-4DDC with the addition of Ag^+ .

3.3. The influence of pH and time

The fluorescence response of TPE-4DDC toward Ag^+ was investigated in $\text{H}_2\text{O}/\text{THF}$ (v/v, 6/4) at different pH values (from 4.2 to 10.1). In the absence of Ag^+ , the fluorescence of TPE-4DDC was rather weak in either acidic or basic solutions. After addition of 5.0 eq. of Ag^+ , the fluorescence intensity was enhanced. Fig. S2 displays that TPE-4DDC can respond to Ag^+ in a wide pH range from 4.2 to 8.8. The fluorescence became much weaker in basic solutions, which could be attributed to the reaction of Ag^+ with OH^- . It is worthwhile to note that the fluorescence emission of TPE-4DDC increased rapidly within seconds in the presence of Ag^+ and reached a stable state in 5 min (Fig. S3), indicating that TPE-4DDC could monitor Ag^+ in real time. Therefore, all measurements of UV-vis absorption and fluorescence were fixed in 10 min and carried out in $\text{H}_2\text{O}/\text{THF}$ (v/v, 6/4) containing HEPES buffer (20 mM, pH = 7.0).

3.4. Selectivity of TPE-4DDC toward Ag^+

The fluorescence behavior of TPE-4DDC was investigated in $\text{H}_2\text{O}/\text{THF}$ (v/v, 6/4) in the presence of various metal ions (5.0 eq.).

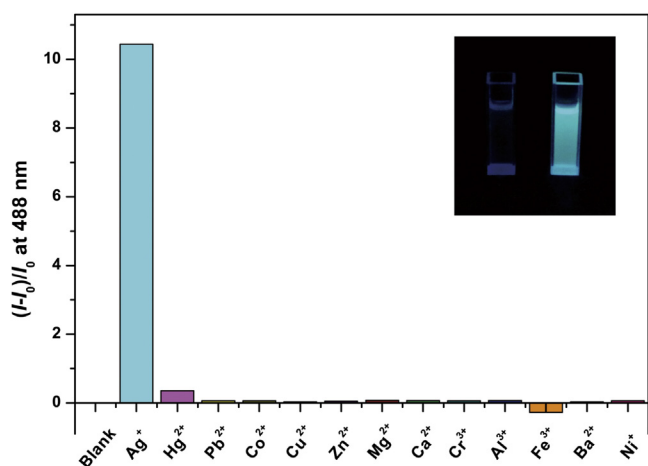


Fig. 4. Fluorescence intensity of TPE-4DDC (40.0 μ M) in the absence and presence of various metal ions Ag^+ , Hg^{2+} , Pb^{2+} , Co^{2+} , Cu^{2+} , Zn^{2+} , Mg^{2+} , Ca^{2+} , Cr^{3+} , Al^{3+} , Fe^{3+} , Ba^{2+} and Ni^{2+} (5.0 eq.) in $\text{H}_2\text{O}/\text{THF}$ (v/v, 6/4) containing HEPES buffer (20 mM, pH = 7.0) ($\lambda_{\text{ex}} = 353$ nm, $\lambda_{\text{em}} = 488$ nm; slit: 1.5 nm, 15 nm). Inset: Fluorescence emission of TPE-4DDC (left) and TPE-4DDC/ Ag^+ (right) under 365 nm UV light illumination.

As shown in Fig. 4, only with addition of Ag^+ , TPE-4DDC exhibited a significant green fluorescence enhancement at 488 nm with an excitation of 353 nm and displayed a large Stokes shift (135 nm). Other metal ions including Hg^{2+} , Pb^{2+} , Co^{2+} , Cu^{2+} , Zn^{2+} , Mg^{2+} , Ca^{2+} , Cr^{3+} , Al^{3+} , Fe^{3+} , Ba^{2+} and Ni^{2+} caused no fluorescence enhancement. Even in the presence of Hg^{2+} , only slight fluorescence alternation could be detected.

Moreover, addition of Ag^+ (5.0 eq.) to the solution of TPE-4DDC containing one of these metal ions (5.0 eq.) led to similar fluorescence enhancement (Fig. 5). Only for Hg^{2+} , the fluorescence intensity decreased by 18%. The possible reason is that a small percentage of intermolecular coordination of TPE-4DDC with Ag^+ was blocked by the desulfurizing reaction between TPE-4DDC and Hg^{2+} . The results clearly indicated that TPE-4DDC exhibited high selectivity toward Ag^+ over most competing ions. Additionally, the fluorescence spectra of TPE-4DDC in the presence of silver salt (5.0 eq.) with different counter-anions (ClO_4^- , CF_3SO_3^- , NO_3^- , BF_4^- , and OAc^-) were measured (Fig. S4). The results reveal that the influence of counter-anions on the detection of Ag^+ with TPE-4DDC is rather minor.

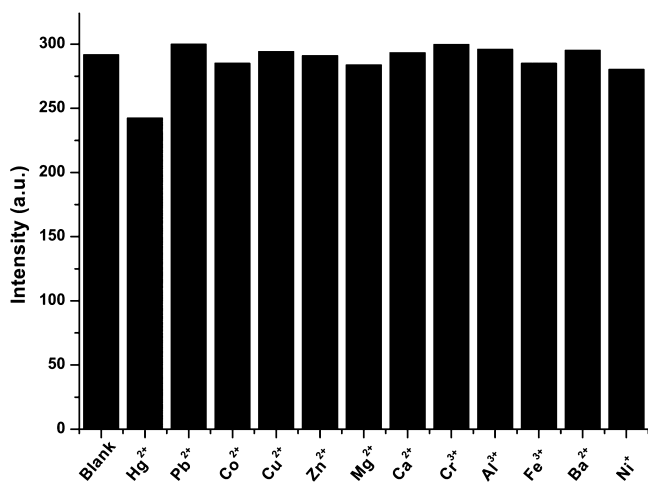


Fig. 5. Fluorescence responses of TPE-4DDC (40.0 μ M) upon addition of Ag^+ (5.0 eq.) in the absence and presence of other metal ions Hg^{2+} , Pb^{2+} , Co^{2+} , Cu^{2+} , Zn^{2+} , Mg^{2+} , Ca^{2+} , Cr^{3+} , Al^{3+} , Fe^{3+} , Ba^{2+} and Ni^{2+} (5.0 eq.) in $\text{H}_2\text{O}/\text{THF}$ (v/v, 6/4) containing HEPES buffer (20 mM, pH = 7.0) ($\lambda_{\text{ex}} = 353$ nm, $\lambda_{\text{em}} = 488$ nm; slit: 1.5 nm, 15 nm).

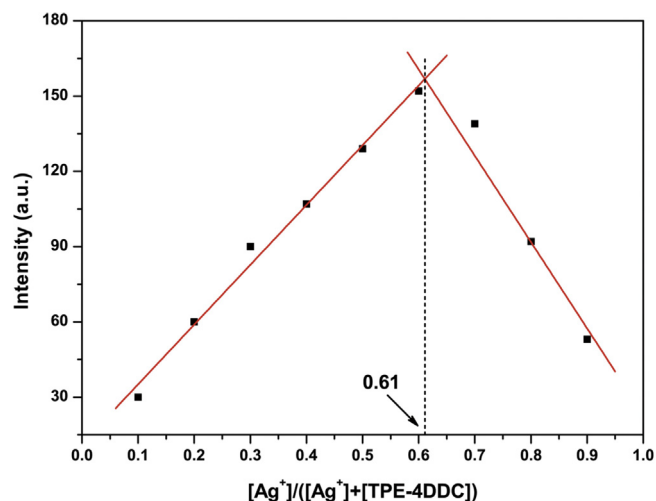


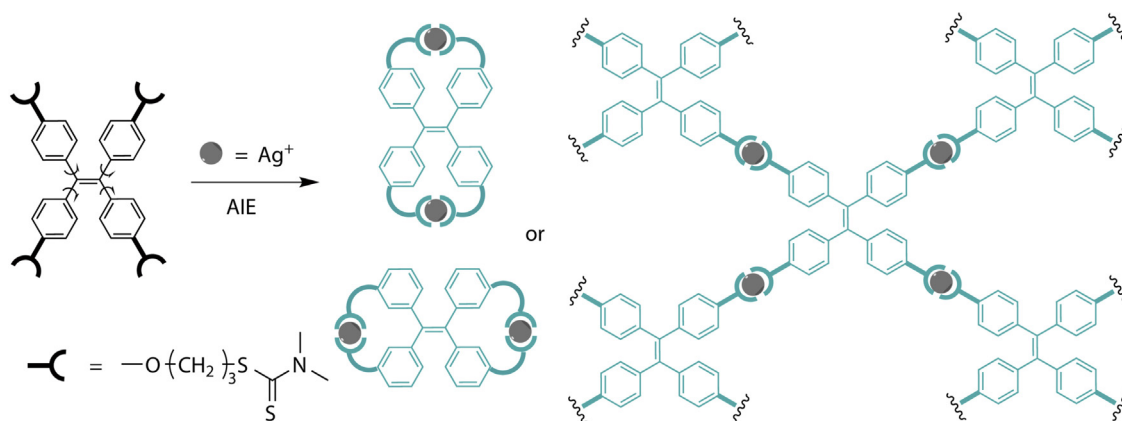
Fig. 6. Job's plot of a 1:2 complex of TPE-4DDC and Ag^+ in $\text{H}_2\text{O}/\text{THF}$ (v/v, 6/4) containing HEPES buffer (20 mM, pH = 7.0, $[\text{TPE-4DDC}] + [\text{Ag}^+] = 40$ μ M ($\lambda_{\text{ex}} = 353$ nm, $\lambda_{\text{em}} = 488$ nm; slit: 1.5 nm, 15 nm).

3.5. Coordination modes between TPE-4DDC and Ag^+

Job's plot experiments were employed to determine the binding stoichiometry of TPE-4DDC and Ag^+ [24,25]. The change of fluorescence intensity at 488 nm with a serial of concentration ratios of TPE-4DDC to Ag^+ is given in Fig. 6. When the molecular fraction of Ag^+ was close to 0.61, the fluorescence intensity reached a maximum. This result indicated that a 1:2 stoichiometry is a possible binding mode of TPE-4DDC and Ag^+ . Further, the spectral titration experiment of AgNO_3 in the presence of different amounts of TPE-4DDC was carried out in $\text{H}_2\text{O}/\text{THF}$ (v/v, 6/4) (Fig. S5). As we predicted, the fluorescence intensity at 488 nm increased almost linearly with the addition of TPE-4DDC in the range of 0–0.5 eq. ($I_{488 \text{ nm}} = 9.52 \times [\text{TPE-4DDC}] + 13.51$, $R^2 = 0.986$, $n = 9$, inset of Fig. S5) and increased by 14 fold when the ratio of $[\text{TPE-4DDC}]/[\text{Ag}^+]$ reached 1:2. Three possible coordination modes of TPE-4DDC with Ag^+ were shown in Scheme 2. Additionally, DLS was employed to study intermolecular coordination of TPE-4DDC with Ag^+ (Fig. S6) [26]. The initial DLS signal corresponding to the species of 55 nm approximately is ascribed to the nanoaggregate formation of TPE-4DDC in $\text{H}_2\text{O}/\text{THF}$ (v/v, 6/4). However, aggregates became larger with the addition of Ag^+ . The result should be attributed to the further aggregation of coordination oligomers and polymers due to their low solubility in $\text{H}_2\text{O}/\text{THF}$ (v/v, 6/4) (Scheme 2).

The ^1H NMR titration in $\text{D}_2\text{O}/\text{THF}-d_8$ (v/v, 6/4) was experimented to further determine the exact binding sites (Fig. 7). The data revealed that the proton signals of the DDC moiety in TPE-4DDC ($\delta = 3.402$, singlet, 3H and $\delta = 3.272$, singlet, 3H assigned to the two $-\text{CH}_3$ groups adjacent to N atom) were shifted downfield and became weaker after the gradual addition of Ag^+ . These obvious downfield shifting effects suggested that there is a decrease in charge density of the methyl, strongly implying that Ag^+ is bound with S in the DDC group due to the strongly thiophilic character of Ag^+ .

Moreover, the restorability of TPE-4DDC was studied by measuring the fluorescence changes with addition of NaCl into a $\text{H}_2\text{O}/\text{THF}$ (v/v, 6/4) solution of TPE-4DDC and Ag^+ [27]. Free TPE-4DDC (1.0 eq.) in solution displayed a very weak fluorescence, while a significant increase of fluorescence was observed with addition of 2.0 eq. of Ag^+ . However, the addition of NaCl (2.0 eq.) in solution of TPE-4DDC and Ag^+ caused an immediate fluorescence decrease. The recovery of fluorescence could be achieved



Scheme 2. Schematic illustration of the coordination modes between TPE-4DDC and Ag⁺.

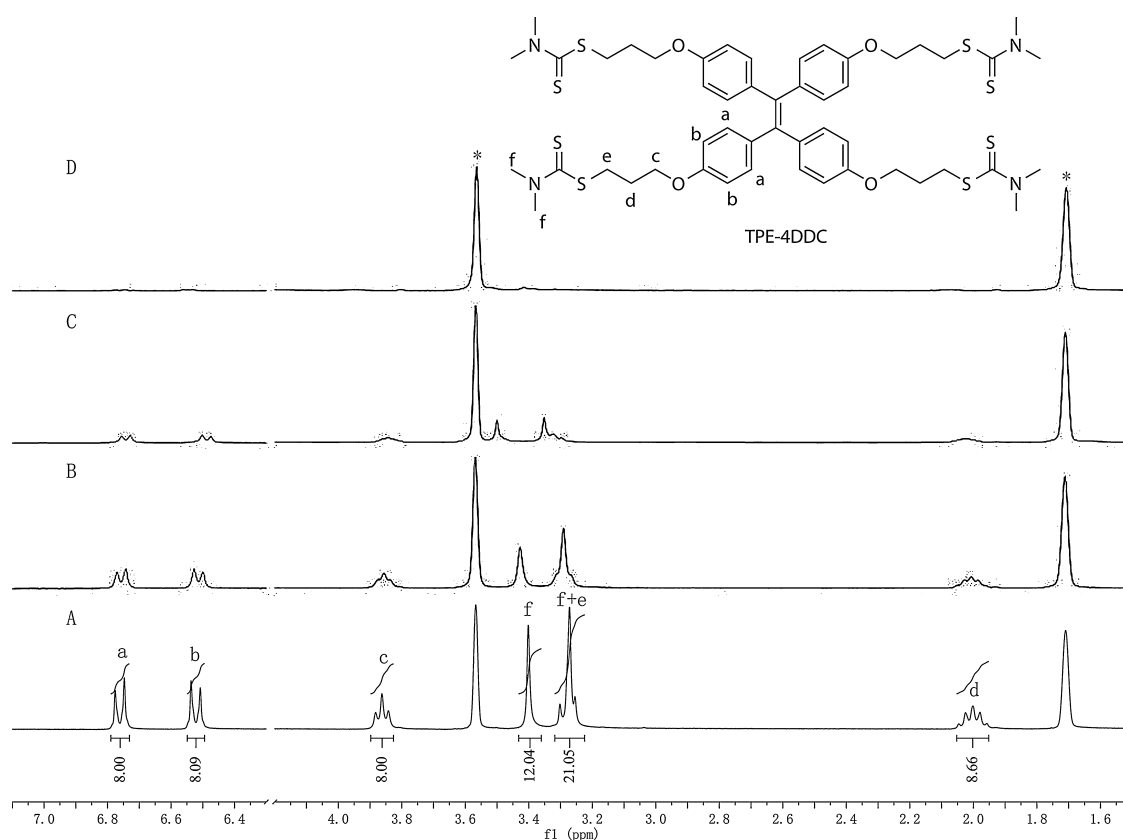


Fig. 7. ¹H NMR spectra (300 MHz, D₂O/THF-*d*₈ (v/v, 6/4)) of TPE-4DDC (5 mM) with the addition of (A) 0 eq., (B) 0.5 eq., (C) 1.0 eq., (D) 2.0 eq. of Ag⁺, (*: solvent peaks of THF).

with further addition of Ag⁺. After 5 cycles, the sensor still showed excellent restorability with little fluorescent intensity loss (Fig. S7). The results indicate that TPE-4DDC could be recovered by addition of NaCl, which is quite useful for developing a resumable sensor.

4. Conclusion

A new “turn on” fluorescent sensor for Ag⁺ with a high selectivity and a large Stokes shift has been developed by taking advantage of the AIE feature of tetraphenylethylene compounds. The ¹H NMR titration and DLS spectra conclude that the binding of DDC with Ag⁺ induces the further aggregation of TPE-4DDC. The fluorescent spectra results indicate that TPE-4DDC can be used as a resumable sensor for Ag⁺ with a detection limit of 8.74×10^{-7} M. Further studies on the development of

“turn on” fluorescent sensors with a high selectivity and their biomedical applications are ongoing in our group.

Acknowledgements

This work was financially supported by the Natural Science Foundation of China (21102187), the Natural Science Foundation of Guangdong Province (S2013010012128) and the Science and Technology Planning Project of Guangdong Province (2012B010200039).

Appendix A. Supplementary data

Supplementary data associated with this article can be found, in the online version, at <http://dx.doi.org/10.1016/j.jphotochem.2014.12.013>.

References

- [1] T.W. Purcell, J.J. Peters, Sources of silver in the environment, *Environ. Toxicol. Chem.* 17 (1998) 539–546.
- [2] M. Álvarez-Corral, M. Muñoz-Dorado, I. Rodríguez-García, Silver-mediated synthesis of heterocycles, *Chem. Rev.* 108 (2008) 3174–3198.
- [3] Y. Sung, S. Wu, Highly selective and sensitive colorimetric detection of Ag⁺ using *N*-1-(2-mercaptoethyl) adenine functionalized gold nanoparticles, *Sens. Actuators B: Chem.* 197 (2014) 172–176.
- [4] C. Liu, S. Huang, H. Yao, S. He, Y. Lu, L. Zhao, X. Zeng, Preparation of fluorescein-based chemosensors and their sensing behaviors toward silver ions, *RSC Adv.* 4 (2014) 16109–16114.
- [5] A. Ceresa, A. Radu, S. Peper, E. Bakker, E. Pretsch, Rational design of potentiometric trace level ion sensors. A Ag⁺-selective electrode with a 100 ppt detection limit, *Anal. Chem.* 74 (2002) 4027–4036.
- [6] Z. Li, L. Zhou, F. Tan, Influence of sample pre-treatment on the determination of trace silver and cadmium in geological and environmental samples by quadrupole inductively coupled plasma mass spectrometry, *Microchim. Acta* 156 (2006) 263–269.
- [7] W. Guo, S. Hu, J. Zhang, H. Zhang, Elimination of oxide interferences and determination of ultra-trace silver in soils by ICP-MS with ion-molecule reactions, *Sci. Total Environ.* 409 (2011) 2981–2986.
- [8] F. Gerondi, M.A.Z. Arruda, Thermospray flame furnace atomic absorption spectrometry for determination of silver in biological materials, *Talanta* 57 (2012) 395–399.
- [9] X. Liu, W. Li, Q. Shen, Z. Nie, M. Guo, Y. Han, W. Liu, S. Yao, The Ag⁺-G interaction inhibits the electrocatalytic oxidation of guanine—a novel mechanism for Ag⁺ detection, *Talanta* 85 (2011) 1603–1608.
- [10] P. Li, H. Zhou, B. Tang, A lysosomal-targeted fluorescent probe for detecting Cu²⁺, *J. Photochem. Photobiol.: A* 249 (2012) 36–40.
- [11] S. Huang, S. He, Y. Lu, F. Wei, X. Zeng, L. Zhao, Highly sensitive and selective fluorescent chemosensor for Ag⁺ based on a coumarin-Se₂N chelating conjugate, *Chem. Commun.* 47 (2011) 2408–2410.
- [12] D. Lin, J. Lai, H. Sun, Z. Yang, Y. Zuo, A turn-on fluorescein spirolactam derivative as a high selective fluorescence probe for detection of silver ion (I) in water, *Anal. Methods* 6 (2014) 1517–1522.
- [13] R.H. Yang, W.H. Chan, A.W.M. Lee, P.F. Xia, H.K. Zhang, K.A. Li, A ratiometric fluorescent sensor for Ag⁺ with high selectivity and sensitivity, *J. Am. Chem. Soc.* 125 (2003) 2884–2885.
- [14] W.Z. Yuan, P. Lu, S.M. Chen, J.W.Y. Lam, Z.M. Wang, Y. Liu, H.S. Kwok, Y.G. Ma, B. Z. Tang, Changing the behavior of chromophores from aggregation-caused quenching to aggregation-induced emission: development of highly efficient light emitters in the solid state, *Adv. Mater.* 22 (2010) 2159–2163.
- [15] V. Bhalla, A. Gupta, M. Kumar, Fluorescent nanoaggregates of pentacenequinone derivative for selective sensing of picric acid in aqueous media, *Org. Lett.* 14 (2012) 3112–3115.
- [16] F. Sun, G. Zhang, D. Zhang, L. Xue, H. Jiang, Aqueous fluorescence turn-on sensor for Zn²⁺ with a tetraphenylethylene compound, *Org. Lett.* 13 (2011) 6378–6381.
- [17] Q.L. Zhao, X.A. Zhang, Q. Wei, J. Wang, X.Y. Shen, A.J. Qin, J.Z. Sun, B.Z. Tang, Tetraphenylethylene modified perylene bisimide: effect of the number of substituents on AIE performance, *Chem. Commun.* 48 (2012) 11671–11673.
- [18] C.W.T. Leung, Y. Hong, S. Chen, E. Zhao, J.W.Y. Lam, B.Z. Tang, A photostable AIE luminogen for specific mitochondrial imaging and tracking, *J. Am. Chem. Soc.* 135 (2013) 62–65.
- [19] B.K. An, S.K. Kwon, S.D. Jung, S.Y. Park, Enhanced emission and its switching in fluorescent organic nanoparticles, *J. Am. Chem. Soc.* 124 (2002) 14410–14415.
- [20] L. Liu, G. Zhang, J. Xiang, D. Zhang, D. Zhu, Fluorescence turn on chemosensors for Ag⁺ and Hg²⁺ based on tetraphenylethylene motif featuring adenine and thymine moieties, *Org. Lett.* 10 (2008) 4581–4584.
- [21] A. Coskun, E.U. Akkaya, Ion sensing coupled to resonance energy transfer: a highly selective and sensitive ratiometric fluorescent chemosensor for Ag⁺ (I) by a modular approach, *J. Am. Chem. Soc.* 127 (2005) 10464–10465.
- [22] K. Shamsipur, M. Alizadeh, C. Hosseini, A selective optode membrane for silver ion based on fluorescence quenching of the dansylamidopropyl pendant arm derivative of 1-aza-4,7,10-trithiacyclododecane ([12] aneNS3), *Sens. Actuators B Chem.* 113 (2006) 892–899.
- [23] L. Wang, W. Qin, X. Tang, W. Dou, W. Liu, Q. Teng, X. Yao, A selective, cell-permeable fluorescent probe for Al³⁺ in living cells, *Org. Biomol. Chem.* 8 (2010) 3751–3757.
- [24] K. Tsukamoto, Y. Shinohara, S. Iwasaki, H. Maeda, A coumarin-based fluorescent probe for Hg²⁺ and Ag⁺ with an *N*'-acetylthioureido group as a fluorescence switch, *Chem. Commun.* 47 (2011) 5073–5075.
- [25] T. Nishimura, S. Xu, Y. Jiang, J.S. Fossey, K. Sakurai, S.D. Bull, T.D. James, A simple visual sensor with the potential for determining the concentration of fluoride in water at environmentally significant levels, *Chem. Commun.* 49 (2003) 478–480.
- [26] D. Xie, Z. Ran, Z. Jin, X. Zhang, D. An, A simple fluorescent probe for Zn (II) based on the aggregation-induced emission, *Dyes Pigments* 96 (2013) 495–499.
- [27] N. Wanichacheva, O. Hanmeng, S. Kraithong, K. Sukrat, Dual optical Hg²⁺-selective sensing through FRET system of fluorescein and rhodamine B fluorophores, *J. Photochem. Photobiol.: A* 278 (2014) 75–81.